Validation of the variational approach for chirped pulses in fibers with periodic dispersion

F. Kh. Abdullaev
Theoretical Division, Physical-Technical Institute, Uzbekistan Academy of Sciences, 700084 Tashkent-84, G. Mavlyanov Str. 2-B, Uzbekistan

J. G. Caputo
Laboratoire de Mathématique, Institut National de Sciences Appliquées de Rouen et Unité CNRS 60-85, Boîte Postale 8, 76131, Mont Saint Aignan Cedex, France

(Received 26 January 1998)

We consider the propagation of chirped optical solitons in a fiber with periodic dispersion and describe this by a variational approach assuming a single pulse ansatz. We obtain a good agreement between the variational equations and the full numerical solution for the low-frequency region below the fundamental resonance. In that case we study the nonlinear resonances and chaotic oscillations of the pulse width and with this analysis we can predict the stochastic decay of pulses under a periodic modulation of the dispersion. For the main resonance and resonances above it, this simple variational approach fails because of a strong emission of linear waves. Then the numerical solution decays slowly while the simple model predicts a fast breakup. In the high-frequency limit the pulse is stable and we can describe it via averaged variational equations for its width and chirp, which we derive. We show that this dynamical model yields interesting physical estimates for soliton propagation in a fiber with dispersion management. [S1063-651X(98)12110-4]

PACS number(s): 42.65.Tg, 42.50.Ar, 42.81.Dp

I. INTRODUCTION

The influence of the modulation of optical fiber dispersion on soliton propagation has attracted a lot of attention recently. In particular, a strong modulation of the dispersion makes it possible to achieve a high bit rate in long optical communication lines [1,2] because it allows us to approach the zero dispersion limit where optical pulses do not interact strongly with one another. Another great advantage of such systems as shown in [3–5] is that the modulational instability is strongly reduced both in bandwidth and in gain. However, the periodic modulation of dispersion leads to the radiative damping of solitons [6,7] or to the existence of vibrating solitons [8] and splitting of solitons [9]. The quasistationary propagation of a localized nonlinear wave in such an inhomogeneous medium is possible, but such a wave is not a soliton in ordinary terms, due to the strong modulation of dispersion a significant chirp develops. Nevertheless, the pulse appears to be stable in many numerical simulations as in the case of a high-frequency modulation [10]. For the purpose of optical communications it is important to show that these pulses are indeed stable.

Another important issue is the simplified description of these chirped pulses via a variational approach [11,12]. New phenomena appear, such as the nonlinear resonances that can occur between the oscillations of the amplitude and width of the soliton and the modulation of the dispersion or the nonlinearity [8,13]. This problem corresponds to the motion of an equivalent particle with variable mass in a periodically varying Kepler potential. The authors of [8] studied these ordinary differential equations (ODE's) and showed numerically that chaotic oscillations existed for some values of the amplitude of the modulation of dispersion and soliton width. They also found numerically the critical amplitude modulation that causes the decay of the soliton. Another study by one of the authors [14] showed that the soliton could break up in the presence of noise and estimated its lifetime. More generally, in works concerning the chaotic dynamics of solitons under periodic perturbations [15,16] it is usually assumed that the soliton exists as a whole and that its parameters such as position and amplitude vary in time in a chaotic fashion. This is not always the case, in particular, when radiation is present or when resonances occur. Then the solutions of the partial differential equation (PDE) and the variational ODE might disagree, as for the massive Thirring model [17].

In this work we have considered the case of a periodically modulated dispersion and computed simultaneously the solution of the partial differential equation and of the variational equations in order to show the correspondence that can be established between the two systems in parameter space. We are not looking for an exact correspondence in the evolution but for a more general agreement over wide regions of phase space and parameter space when extracting the main features such as the width and chirp of the soliton from the full numerical simulations. When the modulation frequency Ω varies, we find three main regions depending on the ratio Ω/ω_0, where ω_0 is the main frequency associated with the oscillation of the soliton width. For $\Omega<\omega_0$ we obtain a good agreement between the PDE and ODE phase spaces and can predict the soliton breakup observed in [9] via a stochasticity criterion on the Hamiltonian associated to the ODE. When $\Omega\geqslant\omega_0$ the ansatz fails because of the emission of radiation by the soliton. This emission diminishes as Ω increases past ω_0 so that one can recover a correspondence for the case of a rapidly varying modulation. In that case a perturbation analysis yields averaged variational equations, which provide a good insight into the physics of the problem. The study completes the picture of [7] by showing that the soliton exhibits a rapid decay for large amplitude modulation. We also give a quantitative mechanism for this decay that explains the results of [9] and extend the approach of [8] by examining the validity of the variational approach over the whole range of modulation frequencies.

At this point it should be noted that many of the conclusions obtained for the periodic dispersion case carry on to the situation where the nonlinearity is periodically modulated. This can be seen by making a change of variable on the nonlinear Schrödinger equation, it holds as long as the modulation is not strong enough to cancel the dispersion. Another situation where this study is of interest is the case of the propagation of a spatial soliton in a medium with a periodic diffraction in the direction of propagation.

The paper is organized as follows: Sec. II describes the model and the main features of the variational ODE. In Sec. III we compute the numerical solution of the perturbed nonlinear Schrödinger equation and compare its main features with the ones given by the variational ODE in order to validate the latter. Here we identify the two main regions where the simple model holds. Section IV shows how one can obtain a criterion for chaos and soliton breakup in the subharmonic region by examining the nonlinear resonances for the Hamiltonian associated with the ODE. The case of a rapidly varying periodic dispersion is addressed in Sec. V. There we derive averaged equations for the pulse width and chirp and show their relevance to the description of the solution of the partial differential equation. Section VI contains our concluding remarks.

II. DESCRIPTION OF THE MODEL

Let us consider the propagation of optical pulses in optical fibers with a periodically varying dispersion. The governing equation is a modified nonlinear Schrödinger equation (NLSE) for the dimensionless envelope of the electric field,

$$iu_x + \tfrac{1}{2} f(x) u_{tt} + |u|^2 u = 0, \tag{1}$$

where x,t are the coordinates along the direction of propagation and time given in a moving reference frame, respectively. The function $f(x)$ describes the periodic modulation of dispersion.

Different types of modulation have been studied, such as, for example, the periodic box modulation [18]. Here we consider the simple model of a one harmonic modulation $f(x) = 1 + f_0 \sin \Omega x$, where f_0 will be in general smaller than 1. The period of the oscillations of dispersion is $L = 2\pi/\Omega$ and should be compared to the dispersive length, which is the characteristic scale associated with a soliton. Frequently authors have considered the case when the dispersive length is much larger than the other scales. Then the guiding-center soliton concept [19] is valid. When the dispersive length is compatible with L, other approaches are necessary. This discussion for a pure soliton carries down to a chirped pulse for which the scale of internal oscillations is defined by a combination of the initial chirp and deviation from the solitonic solution. For picosecond pulses this period is very large but for subpicosecond pulses it may be reduced to a few meters. When this period is of order L we can await resonance phenomena in the propagation of chirped solitons. The considerations performed in this work also concern the case of spatial solitons in inhomogeneous media. For that, change variables $x \to z$, $t \to x$ and assume a periodic modulation of the nonlinear part of the refraction index along the z axis.

Before describing the variational approach we briefly discuss the conserved quantities associated with Eq. (1). Following the method used by Karpman [20] we can show that the number of particles $2N^2 \equiv \int_{-\infty}^{+\infty} |u|^2 dt$ and the momentum $\mathcal{P} = (i/2)\int_{-\infty}^{+\infty}(u_t u^* - u_t^* u)dt$ are constants of the motion for Eq. (1). The Hamiltonian is not preserved and its evolution is given by $d/dx[\int_{-\infty}^{+\infty}(|u|^4 - |u_t|^2)dt] = -2[f(x) - 1]\int_{-\infty}^{+\infty} \mathrm{Im}(u_t^2 u^*)dt$. Because of the conservation of momentum the pulse can be assumed to be at rest so that the position and velocity variables can be ignored. We will calculate the number of particles, momentum, and energy during the computations as a check.

Let us now recall the variational description of a chirped soliton [12],

$$u(x,t) = A(x)\,\mathrm{sech}\left[\frac{t}{a(x)}\right]\exp[ib(x)t^2], \tag{2}$$

where $A(x)$, $a(x)$, and $b(x)$ describe the complex amplitude, width, and soliton frequency chirp, respectively. The evolution of these variables is given by [8]

$$b(x) = \frac{(\ln a)_x}{2 f(x)}, \tag{3}$$

$$(a|A|^2)_x = 0, \tag{4}$$

$$a_{xx} = \frac{4f^2}{\pi^2 a^3} - \frac{4N^2 f}{\pi^2 a^2} + \frac{a_x f_x}{f}, \tag{5}$$

$$(\arg A)_x = -\frac{f(x)}{3a^2} + \frac{5}{6}\frac{N^2}{a}, \tag{6}$$

where N^2 is the conserved quantity associated with the number of particles,

$$\int_{-\infty}^{\infty} |u|^2 dt = 2a|A|^2 \equiv 2N^2. \tag{7}$$

From the system above it can be seen that the equation for a is independent from the others. We can write it using as new coordinates (a,b)

$$a_x = 2abf(x),$$

$$b_x = \frac{2f(x)}{\pi^2 a^4} - 2b^2 f(x) - \frac{2N^2}{\pi^2 a^3}. \tag{8}$$

As can be seen from Eq. (5) the soliton width evolution is described by the motion of an effective particle of variable mass $m = 1/f(x)$ in the nonstationary effective anharmonic potential U [8],

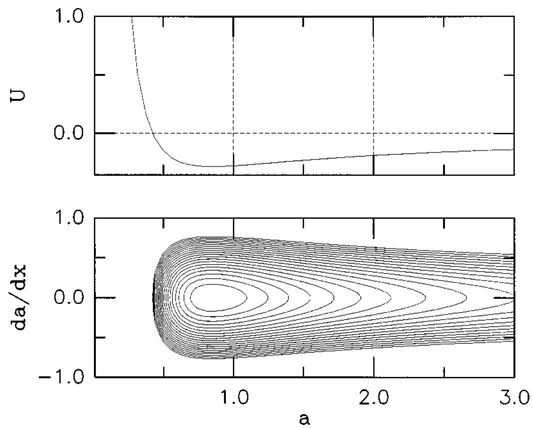

FIG. 1. Potential (11) and phase portrait (a,a_x) associated to the Kepler problem (9) for $N^2=1.18$.

$$\frac{d}{dx}\left[\frac{1}{f(x)}\frac{da}{dx}\right]=-\frac{\partial U}{\partial a},\qquad(9)$$

$$U(a,x)=\frac{2f}{\pi^2a^2}-\frac{4N^2}{\pi^2a},$$

and the Hamiltonian is

$$H(a,a_x,x)=\frac{1}{f(x)}\frac{(a_x)^2}{2}+U(a,x).\qquad(10)$$

At this point it should be mentioned that Eqs. (5) and (8) present a singular behavior when the amplitude of the modulation f_0 is greater than 1. Then the mass of the effective particle goes to 0 so that its speed under the influence of forcing tends to infinity. For the soliton this means that its width goes to 0 and its chirp to infinity.

When $f(x)$ is a periodic function we deal with a periodically perturbed Kepler problem. Consequently, the investigation of the oscillations of the soliton width under the periodic dispersion is reduced to the study of the dynamics of a particle of variable mass in a periodically perturbed Kepler problem. Before proceeding to the solution we will first discuss the unperturbed Kepler problem. We give here the information necessary for further analysis [21,22]. The potential energy is expressed by

$$U=\frac{2}{\pi^2a^2}-\frac{4N^2}{\pi^2a}.\qquad(11)$$

The minimum of this potential is achieved at $a_c=1/N^2$ and is equal to $U_c=-2N^4/\pi^2$. From Eq. (11) the frequency ω_0 of small oscillations of the particle near the bottom of the potential can be found. The result is $\omega_0=2N^4/\pi$. It is the frequency of oscillation of the width of a chirped soliton during its propagation in the homogeneous fiber. Figure 1 shows the potential (11) together with the associated phase portrait (a,a_x) obtained for $N^2=1.18$. The character of the oscillations of the width and amplitude of the soliton is defined by the initial total energy $E_0=2/\pi^2a_0^2-4N^2/\pi^2a_0+2a_0^2b_0^2$. When $E_0<0$, i.e., $1+2\pi^2a_0^4b_0^2<2N^2a_0$ we have an oscillatory regime, but the case $E_0>0$, i.e., $1+2\pi^2a_0^4b_0^2>2N^2a_0$ corresponds to an unbounded motion for which the width of the soliton increases indefinitely indicating that it will be destroyed $(a\to\infty)$. The orbit separating these two types of motion corresponds to $E_0=0$ and is unbounded. Notice also how all orbits get very close to the left of the fixed point, which corresponds to the pure soliton behavior $(a_c,0)$. Therefore we expect that in the presence of a perturbation, a stochastic layer will be generated so that orbits will get mixed at that point leading to escape.

Below we will investigate the case when the first condition $(E_0<0)$ is valid. From Eq. (11) the total energy of the effective particle is

$$E=\frac{a_x^2}{2}+\frac{2}{\pi^2a^2}-\frac{4N^2}{\pi^2a}.\qquad(12)$$

For the oscillatory regime $(E<0)$ the action variable is

$$J=\frac{1}{2\pi}\oint a_x dx=\frac{2\sqrt{2}N^2}{\pi^2\sqrt{-E}}-\frac{2}{\pi}.\qquad(13)$$

The total energy is expressed in terms of the action J by relation

$$H=E=-\frac{8N^4}{\pi^2}\frac{1}{(\pi J+2)^2}.\qquad(14)$$

From this expression we can derive the frequency of oscillations of the soliton width

$$\omega(J)=\frac{dH}{dJ}=\frac{16N^4}{\pi}\frac{1}{(\pi J+2)^3}$$
$$=\frac{\pi^2}{\sqrt{2}N^2}(-E)^{3/2},\qquad(15)$$

which reduces to ω_0 when J goes to zero or $E=U_c$.

We also need to know the spectral properties of the trajectories of the Kepler motion [21]. The orbits are given in parametric form:

$$a=\bar{b}(1-e_0\cos\xi),\quad \omega x=\xi-e_0\sin\xi,\qquad(16)$$

where $e_0=[1-(\pi^2|E|/2N^4)]^{1/2}$ is the eccentricity and $\bar{b}=2N^2/\pi^2|E|$. From Eq. (16) it follows that $a_{min}=\bar{b}(1-e_0)$ and $a_{max}=\bar{b}(1+e_0)$ in agreement with [12]. For further analysis it is important to know the cutoff frequency above which the energy in the power spectrum for the unperturbed motion can be neglected. This gives a number of active harmonics N_0,

$$N_0=(1-e_0^2)^{-3/2}=\frac{2^{3/2}N^6}{\pi^3|E|^{3/2}}.\qquad(17)$$

III. NUMERICAL SIMULATIONS FOR THE VALIDITY OF THE VARIATIONAL APPROACH

In this section we will proceed to compare in detail the long term evolution of the PDE solution with that of the

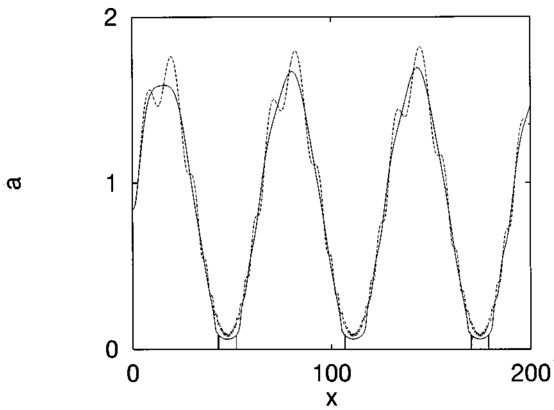

FIG. 2. Variation of the width $a(x)$ for $\Omega=\omega_0/9\, f_0=0.5$, and $N^2=1.2$. The PDE solution is in full lines and the ODE in dashed lines.

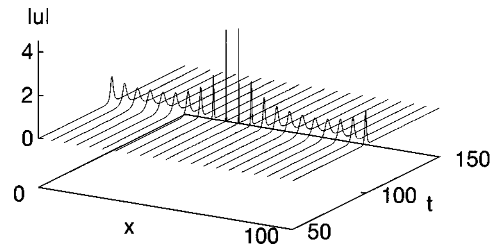

FIG. 4. Three-dimensional plot of the PDE solution for the calculation shown in Fig. 2.

variational ODE's [Eq. (8)]. This is an essential step to establish the validity of this simplified model, which cannot be done *a priori* using analysis. We have concentrated on a comparison of the behaviors of the two systems in terms of the width a and chirp b for long times and also in parameter space. Throughout the computations we have fixed the initial number of particles $N^2=1.18$ for the pulse and therefore the natural frequency of oscillation of the soliton width and varied systematically the forcing frequency Ω over a wide range.

The investigation of the ODE's for the first few low resonances has been performed in [8] and detailed numerical computations of the NLSE have been carried out in [9] for the slow modulation case $\Omega<\omega_0$ and have shown the existence of regions in the parameter space (N^2,f_0) where soliton splitting occurs, and also the presence of islands of stability. Here we complete this picture by estimating the width a and chirp b from the numerical solution and validate the variational approach. Such a comparison was given in [10] for the limiting case where the nonlinearity is negligible and for a large frequency of modulation in the dispersion management scheme.

The numerical method that we have used is the method of lines where the solution of Eq. (1) is advanced in x via an ODE solver and the temporal part of the operator is discretized using finite differences. Using an ordinary differential equation solver gives the scheme an implicit character, that prevents the notorious instabilities that are present when the scheme is explicit in x. The ODE solver that we have used is the DOPRI5 method of Dormand and Prince, analyzed in [23]. This method is a combined fourth- and fifth-order Runge-Kutta-Fehlberg method enabling step size control. This feature is very important because of the periodic perturbation; it guarantees that the step is always adapted to the solution. The tolerance chosen for the integrator is 10^{-6}. The time discretization is done using centered finite differences making the scheme second order. We have chosen for all the results presented 1200 discretization points in t and a window of size 200. To prevent artificial reflections of the waves emitted by the pulse, we have surrounded the computational domain by absorbing layers where an artificial damping, smoothly increasing with t, has been introduced. This damping has been adjusted so that the value of the solution at each end of the domain is approximately 10^{-5}. We are therefore sure that no significant reflection takes place at these boundaries.

The accuracy of the computations is monitored by checking the conservation of the number of particles, the momentum and the energy relation given above. For all cases the momentum is conserved to the accuracy of 10^{-10}. The number of particles is conserved to a very good accuracy up to the point where waves start leaving the computational domain and enter the absorbing layers.

The width a and chirp b were estimated from the numerical solution of the PDE in the following way. Using the modulus of the solution around the pulse down to 20% of its

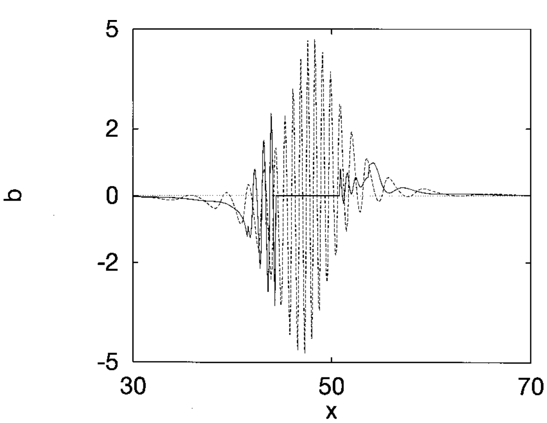

FIG. 3. Variation of the chirp $b(x)$ for the same conditions as for Fig. 2.

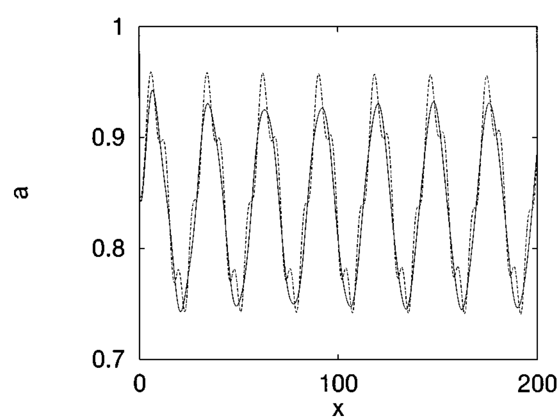

FIG. 5. Variation of the width $a(x)$ for $\Omega=\omega_0/4$ and $f_0=0.1$ for the PDE solution shown in full lines and the ODE in dashed lines.

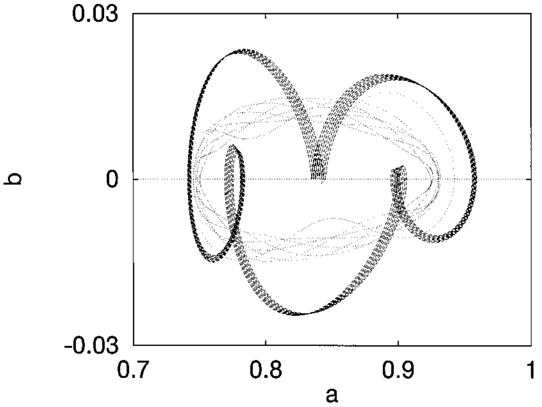

FIG. 6. Phase portrait (a,b) for $\Omega=\omega_0/4$ corresponding to Fig. 5. The orbit corresponding to the PDE is given in dots while that for the ODE is in dashed lines.

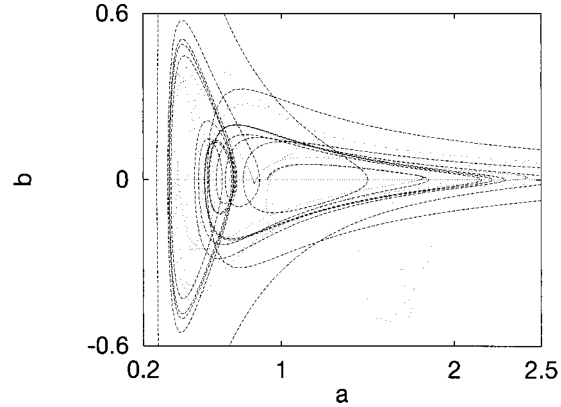

FIG. 8. Phase-portrait (a,b) for $\Omega=\omega_0/4$ corresponding to Fig. 7. The orbit corresponding to the PDE is given in dots while the one for the ODE is in dashed lines.

maximum amplitude we have solved a nonlinear least square problem assuming the chirped soliton form (5) and used a standard conjugate gradient method [24] to obtain the solution. The chirp was estimated by a least square fit on the phase of the solution assuming that it has a quadratic dependance in t.

We first consider the case of a very slow modulation of the dispersion $\Omega=\omega_0/9$. Figure 2 shows the evolution of the width of the pulse $a(x)$ for the PDE and the variational ODE's (5) for a forcing amplitude $f_0=0.5$. We can see the very good agreement between the solution of the partial differential equation (1) and the ODE solution except that the latter contains more harmonics. These oscillations increase in frequency as the ''bottom'' of the modulation curve is reached, there the chirp becomes very large as expected from Eq. (5). Figure 3 shows the chirp $b(x)$ around the minimum of the dispersion for both the PDE (full line) and the ODE (dashed line). The frequency increase is very apparent on the ODE data and less on the PDE for which the fitting routine breaks down at the minimum. The three-dimensional (3D) solution shown in Fig. 4 shows that the pulse becomes compressed very strongly at that point and radiation is emitted. This is mostly a numerical problem as can be seen by doubling the number of discretization points from 1200 to 2400.

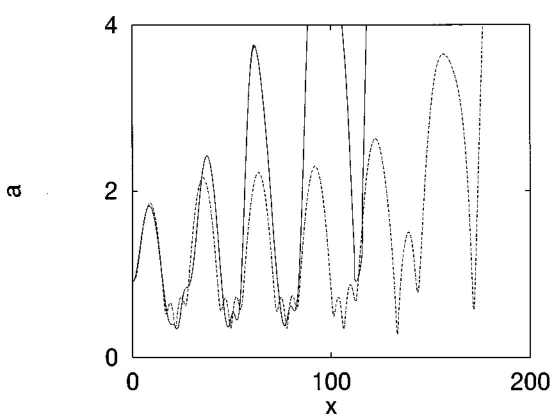

FIG. 7. Variation of the width $a(x)$ showing breakup of the soliton for $\Omega=\omega_0/4$ and $f_0=0.6$ for the PDE solution shown in full lines and $f_0=0.5$ for the ODE solution shown in dashed lines.

Then the small ripples occurring when the pulse is highly compressed, disappear. The increase of the frequency is connected to the adiabatic invariant H/Ω [21] for the equivalent particle oscillating in the potential well. As the dispersion is decreased, the energy of the effective particle representing the pulse is increased because the potential well gets deeper so that in order for the ratio to be constant the frequency should increase.

We now consider the case when the modulation frequency is equal to $\omega_0/4$ and find a good correspondence for $a(x)$ for $f_0=0.1$ as shown in Fig. 5. Again the ODE solution exhibits more harmonics than the PDE solution. This is very apparent on the phase portrait (a,b) shown in Fig. 6 which also shows that the two solutions are very close. When the amplitude of the forcing is increased we observe that a becomes unbounded both for the PDE for $f_0=0.6$ and the ODE for $f_0=0.5$. The evolution of a for these two situations is presented in Fig. 7, where one can notice the good agreement between the two systems even for the higher harmonics. The phase portrait (a,b) for the two systems presented in Fig. 8 is typical of the Kepler problem with the bunching of orbits for small a and the sharp turn for large a. The blowup for $a(x)$ corresponds to the splitting of the pulse into two small pulses as is shown in Fig. 9 and was observed in [9]. Because of the conservation of momentum the small pulses travel with opposite velocities. The good agreement between the variational ODE and the PDE solution is preserved when $\Omega=\omega_0/2$ and we observe breakup of the soliton for $f_0=0.4$ $(f_0=0.3)$ for the PDE (ODE) solution with a good global agreement in the (a,b) phase-space as shown in Fig. 10.

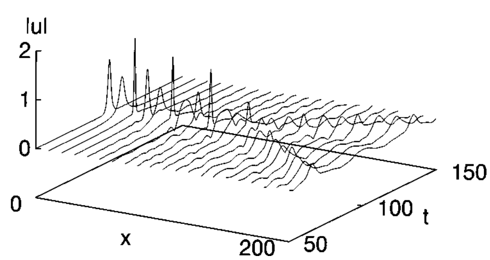

FIG. 9. Three-dimensional plot of the PDE solution corresponding to Figs. 7 and 8 showing the splitting of the soliton into two smaller pulses.

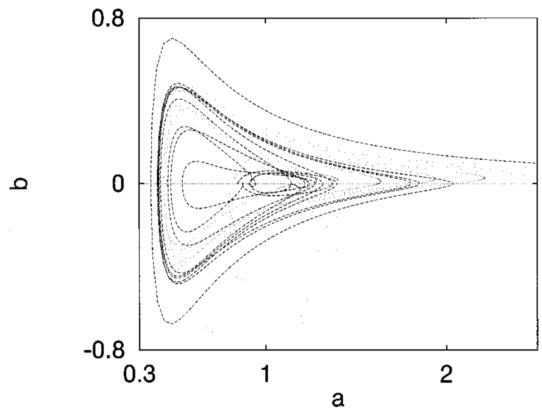

FIG. 10. Phase-portrait (a,b) for $\Omega=\omega_0/2$ and $f_0=0.4$ for the PDE solution shown in dots and $f_0=0.3$ for the ODE solution shown in dashed lines.

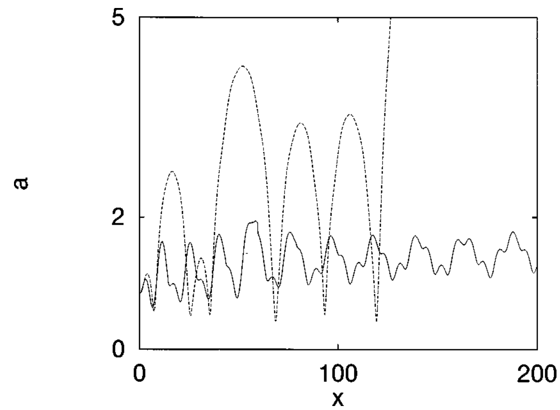

FIG. 12. Variation of the width $a(x)$ for $\Omega=\omega_0$ and $f_0=0.2$ for the PDE solution shown in full lines and the ODE in dashed lines.

When the modulation frequency Ω is increased and reaches ω_0 a resonance occurs for the chirped soliton. Figure 11 shows a plot of the PDE solution for $f_0=0.2$. It shows that the pulse initially adjusts to the perturbation but very quickly develops a strong background of radiation. It will continue to emit and slowly decay as x increases. This resonance value $\Omega=\omega_0\equiv 2N^4/\pi$ between the width a and the chirp b is smaller than $\omega^*=N^4$, the one for a pure soliton calculated using the inverse scattering transform [6,7]. In other words, a soliton will break up for a smaller modulation frequency than expected from IST considerations because it will develop a chirp that will resonate with its width. In this case the description of the chirped pulse via the variational ODE's fails as shown in Fig. 12, which gives the evolution of a for the PDE solution and the ODE for the same parameters as Fig. 11. The ODE solution indicates a complete decay of the soliton after four oscillations while the PDE solution shows a 10% decay over the same period of time. Notice, however, the good agreement between the two curves obtained for $x<5$ which is consistent with the initial evolution of the pulse in Fig. 11. As expected from IST considerations [7] the rate of decay of the pulse due to emission decreases as Ω increases past ω_0. Figure 13 shows the evolution of a for the PDE and the ODE for $\Omega=2\omega_0$ and $f_0=0.2$. The ODE solution escapes to infinity as was predicted in [8], while the PDE solution decays slower than for the main resonance.

The overall correspondence between the PDE and the variational ODE can be seen by examining if the radiation remains in the vicinity of the pulse. For that we compute the evolution of the number of particles inside the computational domain $M=\int_{20}^{180}|u|^2dt$ as a function of x. This is shown in Fig. 14 for different values of the ratio Ω/ω_0. We observe almost no decay for the subharmonic forcing, which suggests that the radiation remains locked to the pulse. On the other hand, there is a fast decay for the fundamental resonance as can be expected from the 3D picture Fig. 11. As expected from [7], the emission of linear waves by the soliton and the decay rate of its amplitude is maximum for $\Omega=\omega_0$ and as Ω is increased, this rate is reduced. It is therefore expected that a simplified description will hold for very large frequencies for which the emitted radiation would be negligible. Indeed a simple model based on the Kapitsa averaging will be presented in Sec. V and shown to be in good agreement with the PDE. Another indication of this agreement is the fact that the stochastic layer becomes exponentially narrow for large frequencies as will be shown in the next section.

To conclude this section, we present in Table I the main results in the comparison between the PDE solution and the variational ODE. We have observed a very good correspondence between the PDE solution and the solution of the variational ODE [Eq. (5)] for close values of the forcing amplitude f_0 as long as $\Omega<\omega_0$. An important consequence of this is that one can establish a criterion for soliton splitting for the PDE by analyzing the perturbed Hamiltonian system (5) for orbits that are close to the separatrix, which corresponds to an unbounded motion. This is the object of the next section.

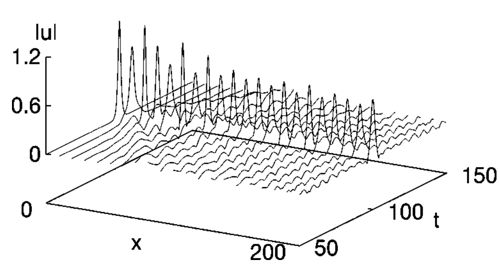

FIG. 11. Three-dimensional plot of the PDE solution for $\Omega=\omega_0$ and $f_0=0.2$.

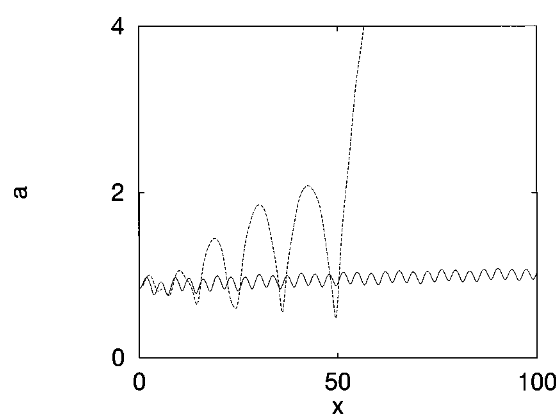

FIG. 13. Same as Fig. 12 except that $\Omega=2\omega_0$.

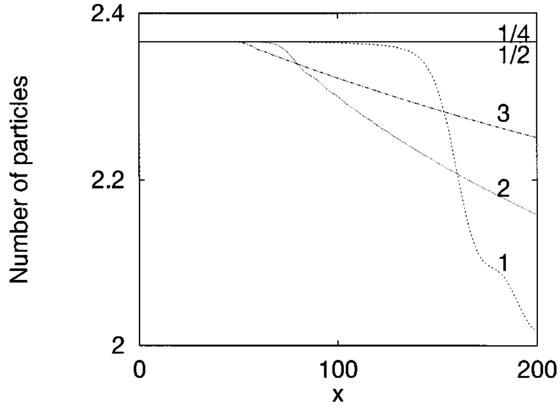

FIG. 14. Evolution of the number of particles in the computational domain $\int_{20}^{180}|u|^2 dt$ for different values of the ratio Ω/ω_0 and an amplitude of the modulation $f_0=0.1$.

IV. NONLINEAR RESONANCES AND CHAOS IN THE SOLITON WIDTH AND AMPLITUDE OSCILLATIONS

During the propagation of chirped soliton in optical fibers there is an interplay between two periodic processes—the soliton width oscillations and the periodic modulation of the fiber dispersion—so that nonlinear resonances and dynamical chaos phenomena are possible. Bearing in mind though that the chaotic motion in the given system is a transient process, the effective particle will obtain in the diffusion process over resonances, a sufficient amount of energy to be freed from the potential well and move as a free particle to infinity. For this reason we can consider the stochasticity criterion that we obtain [Eq. (28)] as a condition for the breaking of the optical soliton. This problem has an interesting close analogy with the problem of the stochastic ionization of a hydrogen atom in a periodic field [25] where an electron escapes from the central potential under a strong periodic electromagnetic field. Then the equation is very similar to Eq. (5) except that the modulation is linear in a due to the field dipole interaction.

For the purpose of analysis the theory of nonlinear resonances [26–28] will be applied. Then it is convenient to use the action-angle variables for the solution of the problem. The total Hamiltonian in the action-angle variables J,θ has the form

$$H=H_0+f_1(x)V=H_0(J)+H_1(J,\theta;x), \tag{18}$$

where the unperturbed Hamiltonian H_0 is given by Eq. (14) and the interaction term H_1 of the Hamiltonian in the approximation $f=1+f_1$, $f_1\ll 1$ is

$$H_1(J,\theta;x) = f_1(x)\left(-\frac{1}{2}(a(J,\theta)_x)^2+\frac{2}{\pi^2 a^2}\right)\equiv f_1(x)V. \tag{19}$$

From Eqs. (18) and (19) we can write the equations of motion using the variables J,θ,

$$\frac{dJ}{dx}=-f_1(x)\frac{\partial V}{\partial \theta},$$

$$\frac{d\theta}{dx}=\omega(J)+f_1(x)\frac{\partial V}{\partial J}. \tag{20}$$

The periodic force $f(x)$ causes nonlinear resonances in the oscillations of the soliton parameters. The regions of nonlinear resonances can be obtained by using the expansion of $V(J,\theta;x)$ in Fourier series in θ. Using Eq. (17) we find from Eq. (19)

TABLE I. Behavior of the solutions of the PDE (1) and the ODE (8) for different forcing frequencies.

$\frac{\Omega}{\omega_0}$	Variational ODE	Nonlinear Schrödinger
	Agreement for $f_0<0.5$, chirp $\lvert b\rvert\to\infty$, width $a\to 0$	
$\frac{1}{16}$		Compressed pulse
$\frac{1}{9}$		No radiation
	Agreement	
$\frac{1}{4}$	$a\to\infty$ for $f_0=0.5$	Soliton break-up for $f_0=0.6$
	Agreement	
$\frac{1}{2}$	$a\to\infty$ for $f_0=0.3$	Soliton break-up for $f_0=0.4$
	Disagreement	
1	$a\to\infty$ for $f_0=0.2$	Radiation 20% decay for $0<x<200$
	Disagreement	
2	$a\to\infty$ for $f_0=0.2$	Radiation 10% decay for $0<x<200$
	Disagreement	
3	$a\to\infty$ for $f_0=0.4$	Radiation 5% decay for $0<x<200$

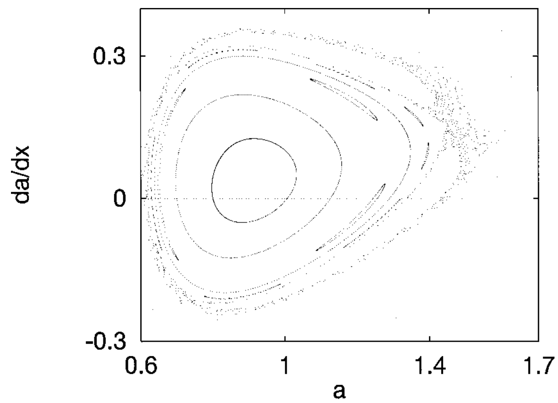

FIG. 15. Poincare section (a,a_x) for the case $\Omega=\omega_0/2$ and a forcing amplitude $f_0=0.1$.

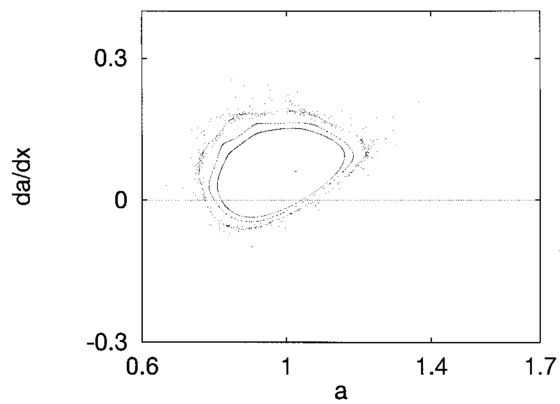

FIG. 16. Same as Fig. 15 for a forcing amplitude $f_0=0.2$.

$$H_1=\sum_{m,k} V_m f_k e^{-im\theta+ik\Omega x}+\text{c.c.}, \tag{21}$$

$$V_m=\frac{1}{2\pi}\int_0^{2\pi} V e^{im\theta} d\theta. \tag{22}$$

Below for simplicity we consider the case when there is only one harmonic term in $f_1(x)=f_0 \sin \Omega x$. Resonances appear when there is an integer m such that

$$m\omega(J)-\Omega=0, \tag{23}$$

i.e., when $\omega=\omega_m\equiv\Omega/m$. The oscillations of the soliton width a and amplitude resonate with the periodical modulations of the fiber dispersion. To our knowledge, the first low nonlinear resonances were investigated in [8]. Notice also that the dynamics of chirped pulses in fibers with random parameters has been studied in [14], where it was shown that randomness can be used for the control of the parameters of the soliton. To investigate the influence of the external periodic action on the character of motion the simplest is to investigate a Poincare section built by sampling an orbit in the phase space (a,a_x) obtained from Eq. (5) every time interval $2\pi/\Omega$.

Figure 15 presents the Poincare section obtained for $\Omega=\omega_0/2$ and $f_0=0.1$. One can see non resonant trajectories slightly deformed corresponding to the KAM theorem. Notice the third-order resonance and the seventh-order resonance just beneath the stochastic layer. The orbits entering this layer eventually escape to infinity. When the forcing parameter is increased to $f_0=0.2$ as shown in Fig. 16 all the nonlinear resonances disappear and the stochastic layer becomes closer to the periodic orbit.

The Hamiltonian (18) corresponds to a system with one degree of freedom and therefore one can apply directly the Chirikov stochasticity criterion [26] where the width of the nonlinear resonance is compared to the separation between resonances. The width of the nonlinear resonance is given by [26]

$$\Delta\omega=2\left|f_0 V_m \frac{d\omega}{dJ}\right|^{1/2}. \tag{24}$$

The distance between resonances is

$$\delta\omega=|\omega_{m+1}-\omega_m|=\frac{\Omega}{m(m+1)}. \tag{25}$$

If we increase the value of the amplitude of the modulation of dispersion f_0 then the width of the resonance will increase and the overlap of neighboring resonances is possible. One condition for this overlap to occur is [26]

$$K=\left(\frac{\Delta\omega}{\delta\omega}\right)^2\geqslant 1. \tag{26}$$

Substituting Eqs. (24) and (25) into Eq. (26) we obtain the stochasticity criterion

$$\frac{4 f_0 V_m w' m^2 (m+1)^2}{\Omega^2}\geqslant 1. \tag{27}$$

From this condition we can find the value of f_0, when chaotic oscillations of the soliton width must occur, i.e.,

$$f_0\geqslant\frac{\Omega^2}{4 V_m \omega' m^2 (m+1)^2}. \tag{28}$$

This is the condition of the appearance of chaos near the mth resonance. So, for almost all initial conditions and parameters of the problem, satisfying condition (28) the oscillations of the soliton width will be chaotic. Note that even in the developed chaos region some regions of regular motion will remain. The Fourier component V_m can be calculated from the equations for a and x in parametric forms (16) and (19), (21), to be

$$V_m=\frac{1}{\pi^3 \bar{b}^2}\int_0^{2\pi}\frac{e^{im(\xi-e_0\sin\xi)}}{1-e_0\cos\xi}d\xi - \frac{\bar{b}^2 e_0^2\omega^2}{4\pi}\int_0^{2\pi}\frac{e^{im(\xi-e_0\sin\xi)}\sin^2\xi}{1-e_0\cos\xi}d\xi. \tag{29}$$

We have computed the integrals in Eq. (29) numerically using the Romberg method because of the oscillating character of the integrands and found the right hand side f_m of the inequality (28) for several values of m. For $\Omega=\omega_0/4$ we find for an initial amplitude $a_0=0.8$ and $N^2=1.18$

$f_1=0.19$, $f_2=0.24$, $f_3=0.76$, and $f_4=3.47$ while for $a_0=0.51$, $f_1=0.16$, $f_2=0.0185$, $f_3=0.0054$, and $f_4=0.002$. This agrees with the numerical observation that the orbit is regular for $a_0=0.8$ and $f_0=0.1$ while it is in the stochastic layer for the $a_0=0.51$. For $\Omega=\omega_0/2$ which corresponds to Figs. 15 and 16, we find for $a_0=0.81$, $f_1=0.74$, $f_2=0.97$, $f_3=3.04$, and $f_4=13.89$ and for $a_0=0.77$, $f_1=0.12$, $f_2=0.097$, $f_3=0.13$, and $f_4=0.54$, which agrees with the observation from the Poincare section that the orbit for $a_0=0.8$ is regular while that for $a_0=0.77$ is chaotic for $f_0=0.2$.

In the limiting case of a large value of m the Fourier component V_m can be estimated by computing the integrals using a form of steepest descent. We obtain

$$V_m \approx \left(\frac{\overline{b^2} e_0 \omega^2 (1-e_0)}{4\pi} + \frac{1}{\pi^3 \overline{b^2}} \right) J_1, \tag{30}$$

where J_1, is given by

$$J_1 \approx \frac{2\sqrt{\pi}}{\sqrt{5}} \frac{1}{\sqrt{m} e_0^{1/4} (1-e_0)^{5/4}} \times \exp\left(1/4 - 5m \frac{(1-e_0)^{3/2}}{6 e_0^{1/2}} \right), \tag{31}$$

from which we can obtain an estimate for the chaos criterion. Near the separatrix, when $E\to 0$, and $\overline{b}\to\infty$ the behavior of V_m is given by

$$V_m \approx \frac{2^{1/4}}{5^{1/2}} \frac{e_0^{3/4} |E|^{3/2}}{\sqrt{\Omega}} \exp\left(\frac{1}{4} - \frac{5}{3\, 2^{5/2}} \frac{\Omega}{\omega_0} \right), \tag{32}$$

so that the oscillations of the width are chaotic when the amplitude of the forcing f_0 is greater than

$$f_{th} = \frac{\pi^3 \sqrt{5}}{3\, 2^{5/4}} \frac{|E|^{5/2}}{\Omega^{3/2} e_0^{3/4} \omega_0} \times \exp\left(-\frac{1}{4} + \frac{5}{3\, 2^{5/2}} \frac{\Omega}{\omega_0} \right). \tag{33}$$

We can therefore use these estimates to predict chaos and the break-up of the soliton. In the region where the initial energy is negative, such that $1+b_0^2\pi^2 a_0^4 > 2N^2 a_0$ where according to the standard analysis a soliton must exist, it breaks up. The main reason consists in a diffusion over resonances and a transition from the oscillatory regime to the unbounded motion where $E>0$. The boundary of the stochastic layer in frequency is obtained by setting the parameter of stochasticity K equal to 1. From Eq. (33) we obtain

$$\overline{\omega} = \frac{3^{3/5} 2^{5/4}}{\pi^{4/5} 5^{3/10}} \frac{\Omega^{9/10} f_0^{3/5}}{\omega_0^{2/5}} \exp\left(\frac{3}{20} - \frac{1}{2^{5/2}} \frac{\Omega}{\omega_0} \right), \tag{34}$$

where ω_0 is defined by Eq. (19). When the initial condition is in the stochastic layer there will be diffusion over resonances and eventually the soliton width will tend to infinity, i.e., the soliton will decay. The boundary frequency of the stochastic layer $\overline{\omega}$ means that for some values of the initial chirp b_0 and width of soliton a_0, i.e., the energy of effective particle E there exists a value of the frequency for which the oscillation will be chaotic.

From the expression for the width of the stochastic layer (34) we observe that when the frequency of perturbation grows the stochastic layer gets exponentially narrow so that the soliton becomes more stable in the high-frequency region. This shows the interest of studying pulse propagation in the case of a rapidly varying dispersion. This is the object of the next section.

V. PROPAGATION OF CHIRPED PULSE IN FIBER WITH RAPIDLY CHANGING DISPERSION

In the case of a high-frequency modulation, the radiation emitted by the pulse is very strongly reduced, we therefore expect a low-dimensional description of the system to hold and we will show that the variational approach can be used to describe the propagation of a chirped pulse in a fiber with a rapidly and strongly changing dispersion. Such a system has been intensively investigated as a perspective for optical communications [1]; an example is the two-step dispersion management scheme with alternating values of the dispersion value giving a nonzero average. Numerical simulations have been carried out in [18] and show that an additional amount of energy is necessary in order to propagate a pulse in such a medium; a formula for this additional energy was suggested. In the recent work [29] this problem has been reduced to the investigation of the properties of a complicated mapping and it was shown that the dynamics is described by the averaged dispersion. Here we follow a different approach and show that the variational approach can explain the main properties of the numerical calculations and gives a formula for the additional energy in agreement with [18].

Assuming as above a sinusoidal variation of the dispersion we perform the averaging of the variational equations (8) over fast oscillations following the Kapitza approach [21]. In this method f_0,Ω are not assumed to be small, but their ratio is small, i.e., $\epsilon=f_0/\Omega \ll 1$. We obtain the slow dynamics via an expansion in powers of ϵ. It should be noted that Eq. (8) should be used for the averaging and not Eq. (5) to eliminate the singular behavior observed for low frequencies. We write the solution of the system (8) in the form

$$a=\langle a\rangle+\delta a, \quad b=\langle b\rangle+\delta b,$$

$$\delta a, \quad \delta b \ll \langle a\rangle, \langle b\rangle, \tag{35}$$

where $\langle a\rangle$ and $\langle b\rangle$ are slowly varying over the distance $1/\Omega$ and the δ are rapidly changing functions. Below we will omit the averaging symbol $\langle\cdots\rangle$. Substituting Eq. (35) into the above mentioned equations for $a(x), b(x)$ we have the following equations for the mean values a,b:

$$a_x = 2ab + 2a\langle \delta b f_1\rangle + 2b\langle \delta a f_1\rangle + 2\langle \delta a\, \delta b\rangle, \tag{36}$$

$$b_x=\frac{2}{\pi^2a^4}\left(1+10\frac{\langle\delta a^2\rangle}{a^2}-4\frac{\langle\delta a f_1\rangle}{a}\right)-2b^2-2\langle\delta b^2\rangle$$

$$-4b\langle\delta b f_1\rangle-\frac{2N^2}{\pi^2a^3}\left(1+\frac{6\langle\delta a^2\rangle}{a^2}\right), \tag{37}$$

and the equations for the corrections $\delta a,\delta b$,

$$\delta a_x=2f_1ab+2a\,\delta b+2b\,\delta a, \tag{38}$$

$$\delta b_x=\left(\frac{6N^2}{\pi^2a^4}-\frac{8}{\pi^2a^5}\right)\delta a+\left(\frac{2}{\pi^2a^4}-2b^2\right)f_1-4b\,\delta b. \tag{39}$$

Let solve these equations assuming for δa and δb a harmonic decomposition, taking into account that the parameter f_0 is large. Keeping the main order terms we obtain the solution

$$\delta a=-\frac{2f_0}{\Omega}\cos(\Omega x)ab-\frac{4f_0}{\pi^2\Omega^2a^3}\sin(\Omega x)$$

$$-\frac{4f_0}{\Omega^2}\sin(\Omega x), \tag{40}$$

$$\delta b=-\frac{2f_0}{\pi^2\Omega}\cos(\Omega x)+\frac{4f_0b}{\pi^2\Omega^2a^4}\sin(\Omega x)$$

$$+\frac{4f_0b^3}{\Omega^2}\sin(\Omega x). \tag{41}$$

Substituting Eqs. (40) and (41) into Eqs. (36) and (37) we obtain the equations for the averaged soliton width and chirp,

$$a_x=2ab+\frac{f_0^2}{\Omega^2}\left(\frac{4b}{\pi^2a^3}-2ab^3\right), \tag{42}$$

$$b_x=\frac{2}{\pi^2a^4}-2b^2-\frac{2N^2}{\pi^2a^3}$$

$$+\frac{4f_0^2}{\pi^2\Omega^2}\left(\frac{12b^2}{a^4}+\frac{3}{\pi^2a^8}-2b^4-\frac{6N^2b^2}{a^3}\right). \tag{43}$$

Equations (42),(43) provide a simple tool to investigate the influence of a high-frequency modulation on a chirped pulse. To examine the validity of the approach we have compared the numerical solution of the PDE [Eq. (1)] with the solution given by the ODE's [Eqs. (42) and (43)]. An important step in solving the latter is to take into account the fact that the correction terms δa and δb in Eqs. (40) and (41) are nonzero when $x=0$. Therefore the initial conditions for Eqs. (42) and (43) for $x=0,(a_0',b_0')$ are given by $b_0'=b_0+(2f_0/\pi^2\Omega)$ and $a_0'=\{a_0/[1-(2f_0b_0'/\pi^2\Omega)]\}$ where (a_0,b_0) are the initial width and chirp for the PDE. Figure 17 shows the evolution of a for $\Omega=15\omega_0$ and $f_0=3$. The PDE solution is in full line, the previous variational ODE [Eq. (5)] solution in dashed line and the averaged ODE solution (42),(43) in short dashed line. As can be seen the pulse width tends towards a constant while both ODE approaches predict oscillations. The value of the fixed point for the PDE about 0.95 is given to a good approximation by the average of the maximum and minimum of the ODE solutions, which is 0.9 assuming $a_0'=0.84$ and $b_0'=0$. The slight underestimation present here is reminiscent of the unperturbed case where the variational ODE gives a periodic soliton width while the PDE shows that the width tends towards a given value. The chirp b is shown in Fig. 18 for the PDE solution in full line and the averaged ODE solution in dashed line. The initial evolution is well approximated for $x<5$.

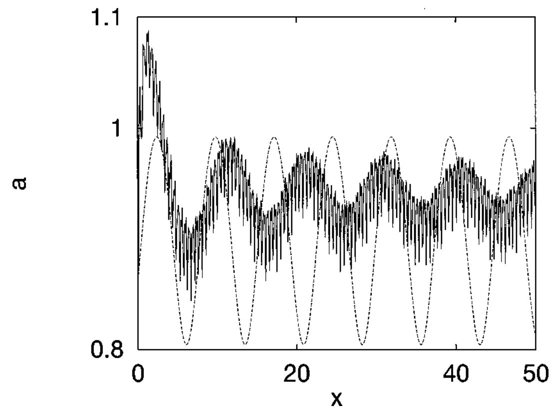

FIG. 17. Variation of the width $a(x)$ for $\Omega=15\omega_0$ and $f_0=3$. The PDE solution is shown in full line and the averaged ODE solution from Eqs. (42) and (43) is drawn in short dash.

We note here that an averaging procedure for the dispersion management scheme has been carried out directly on the PDE [Eq. (1)] and yielded a modified nonlinear Schrödinger equation with higher-order corrections nonlinear in the derivatives [30]. This explains the fact that the PDE solution tends to the fixed point just as in the unperturbed case. An interesting corollary of this work would be to find the field equations corresponding to our averaged system (42),(43) and compare with the ones given in [30].

The system (42),(43) can be written in a more elegant way by using the new variable $\nu=ab$ suggested in [10], which shares with b the property of not having a singular evolution. We have

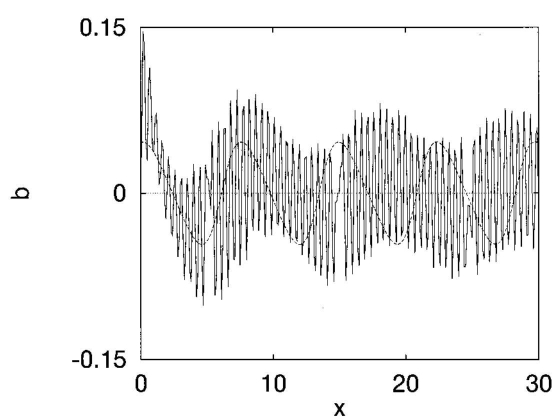

FIG. 18. Variation of the chirp $b(x)$ for the calculation shown in Fig. 17. The PDE solution is shown in full line and the averaged ODE solution from Eqs. (42) and (43) is drawn in short dash.

$$a_x = 2\nu\left[1 + \frac{f_0^2}{\Omega^2}\frac{4}{\pi^2 a^3}\left(\frac{3}{a} - 2N^2\right)\right], \tag{44}$$

$$\nu_x = \frac{2}{\pi^2 a^3} - \frac{2N^2}{\pi^2 a^2} + \frac{f_0^2}{\Omega^2}\frac{12}{\pi^2 a^4}\left[\frac{1}{\pi^2 a^3} + \left(\frac{2}{a} - N^2\right)\nu^2\right]. \tag{45}$$

We can simplify this system by taking into account the smallness of the expansion parameter f_0^2/Ω^2 and obtain

$$a_{xx} = \frac{4}{\pi^2 a^3} - \frac{4N^2}{\pi^2 a^2} + \frac{24 f_0^2}{\pi^4 \Omega^2 a^7} - \frac{6 f_0^2}{\pi^2 \Omega^2 a^4}\left(\frac{2}{a} - N^2\right)(a_x)^2. \tag{46}$$

This describes the motion of a particle in the field of an anharmonic potential depending from the velocity. The fixed point of these equations is given by

$$a = \frac{1}{N^2} + \frac{6N^6 f_0^2}{\pi^2 \Omega^2}, \quad a_x = 0. \tag{47}$$

It corresponds to the minimum of the effective potential

$$U_{eff} = \frac{2}{\pi^2 a^2} - \frac{4N^2}{\pi^2 a} + \frac{4 f_0^2}{\pi^4 \Omega^2 a^6}. \tag{48}$$

Compared with the unperturbed potential (11) we seen that the difference is in the third term in Eq. (48). This addition corresponds to increasing of the short range repulsion. Remembering that this repulsive part of the potential corresponds to the correction of the dispersion, we can conclude that the averaged dynamics corresponds to a uniform fiber with a larger overall dispersion.

The evolution of a chirped pulse in the two step dispersion management scheme can be described by a similar approach except that now the modulation of dispersion has an infinite number of harmonics and using Parseval's relation, f_0^2 in Eqs. (42) and (43) should be replaced by $\Sigma_{m\neq 0}(|c_m|^2/m^2)$, where c_m is the Fourier coefficient of the modulation function $f(x)$. So we obtain at first order the motion of a soliton in a medium with the averaged dispersion value d, which is small and corresponds to the anomalous dispersion case. The corresponding corrections are of the order $\epsilon^2 = f_0^2/\Omega^2$.

In the derivation we consider the propagation of a pulse in a fiber with two segments of alternating dispersions with values d_1 and length l_1 and negative value d_2 with length l_2. We expand such a periodic function $f(x)$ into a Fourier series

$$f(x) = \sum_{n=-\infty}^{+\infty} c_n e^{(i2n\pi x/L)},$$

where $L = l_1 + l_2$. The coefficients are given by

$$c_n = \frac{1}{L}\int_0^L \phi(x) e^{(-i2n\pi x/L)} dx,$$

and they are

$$c_0 \equiv d = \frac{l_1 d_1 + l_2 d_2}{l_1 + l_2},$$

$$c_n = \frac{\Delta d}{2n\pi}\left[\sin\frac{2n\pi l_1}{L} + i\left(\cos\frac{2n\pi l_1}{L} - 1\right)\right], \tag{49}$$

where $\Delta d = d_1 - d_2$.

From the fixed point relation (47) and a time rescaling of the NLSE [Eq. (1)] we obtain a stationary propagation of a pulse of average width a_0 and energy N^2 in a medium of average dispersion d when

$$a_0 = \frac{d}{N^2}\left(1 + \frac{6}{\pi^2}\frac{N^8}{d^6}\frac{f_0^2}{\Omega^2}\right). \tag{50}$$

Compared to the uniform dispersion case $f(x) \equiv d$ such a pulse has a larger width and a smaller amplitude. Therefore one needs additional energy to support it in the rapidly varying case. From the Fourier representation of f and Eq. (50) we find this additional energy to be

$$E = \frac{d}{a_0}\left(1 + \frac{3}{2\pi^4}\frac{(\Delta d)^2}{d^2}\frac{l_1 l_2}{a_0^4}\right). \tag{51}$$

This formula shows that increasing the dispersion difference, or shortening the lengths l_1 or l_2 leads to an increase of this energy. Also the main dependencies in this expression agree with the empirical formula derived in [18] from the numerical simulations.

VI. CONCLUSION

We have performed a validation of the chirped pulse variational approach in the case of a periodically modulated dispersion by comparing systematically the evolution of the PDE solution with the one given by the ODE. We found three main regions of interest depending on the ratio of the forcing frequency Ω to the natural frequency of oscillation of the pulse ω_0. When $\Omega < \omega_0$ the variational approach provides a good model for the description of the soliton. Very little radiation is present. In that case we observe soliton chaos and breakup due to nonlinear resonances. We predict the value for breakup via the Chirikov stochasticity criterion on the variational ODE. When Ω reaches ω_0 a resonance occurs and the soliton emits radiation. In this region, the simplified model fails completely. The emission of radiation is strongly reduced when $\Omega \gg \omega_0$ so that a low-dimensional description is again possible. Also the analysis of the ODE system reveals that increasing the frequency of modulation leads to an exponentially small stochastic layer and thus to a stable pulse.

By averaging a well chosen system of variational equations via the Kapitza approach, we obtain the equations for the mean width and chirp of the pulse. Because the expansion parameter is the ratio of the amplitude of the modulation to the frequency, the former can be large so that the study applies to the case of a dispersion management. The solution of the variational equations is in good agreement with the solution of the PDE. It predicts for example the increased width of the pulse in such a medium. This simple model also yields the additional power necessary to propagate a pulse in a dispersion managed fiber as opposed to a uniform dispersion fiber.

Finally we note that the mechanism of instability in the subharmonic case is universal and independent from the character of periodicity of modulation of dispersion. The results obtained can be applied to analogous problems in the theory of spatial solitons in modulated nonlinear media and for the motion of a body with variable mass in a central potential. In the rapidly varying case the analysis can also be extended to any type of periodicity.

ACKNOWLEDGMENTS

F.A. thanks the INSA de Rouen for its hospitality during the completion of this work. The authors are grateful to S. A. Darmanyan and I. Uzumov for useful discussions and comments. We acknowledge partial support by INTAS (Grant No. 96-0339).

[1] N. J. Smith, F. M. Knox, N. J. Doran, and I. Benion, Electron. Lett. **32**, 54 (1996).
[2] A. Hasegawa, Yu. Kodama, and A. Maruta, Opt. Fiber Technol.: Mater., Devices Syst. **3**, 197 (1997).
[3] N. Smith, and N. J. Doran, Opt. Lett. **21**, 570 (1996).
[4] F. Kh. Abdullaev, S. A. Darmanyan, A. Kobyakov, and F. Lederer, Phys. Lett. A **220**, 213 (1996).
[5] J. C. Bronski and J. N. Kutz, Opt. Lett. **21**, 937 (1996).
[6] J. P. Gordon, J. Opt. Soc. Am. B **9**, 91 (1992).
[7] F. Kh. Abdullaev, J. G. Caputo, and N. Flytzanis, Phys. Rev. E **50**, 1552 (1994).
[8] B. A. Malomed, D. F. Parker, and N. Smyth, Phys. Rev. E **48**, 1418 (1993).
[9] R. Grimshaw, J. He, B. A. Malomed, Phys. Scr. **53**, 385 (1996).
[10] I. Gabitov, E. Shapiro, and S. Turytsin, Phys. Rev. E **55**, 3624 (1997).
[11] D. Anderson, Phys. Rev. A **27**, 3135 (1983).
[12] D. Anderson, M. Lisak, and T. Reichel, J. Opt. Soc. Am. B **5**, 207 (1988).
[13] F. Abdullaev, in *Recent Progress in Optical Solitons in Optical Fibers*, edited by A. Hasegawa (Kluwer, Dodrecht, 1996), p. 91.
[14] F. Kh. Abdullaev, A. A. Abdumalikov, and B. B. Baizakov, Opt. Commun. **138**, 49 (1997).
[15] F. Kh. Abdullaev, S. A. Darmanyan, and P. K. Khabibullaev, *Optical Solitons* (Springer-Verlag, Heidelberg, 1993).
[16] R. Scharf and A. R. Bishop, Phys. Rev. A **46**, R2973 (1993).
[17] D. J. Kaup and T. Lakoba, in *Proceedings of the Gallipoli School on Nonlinear Waves* (World Scientific, Singapore, 1996).
[18] N. J. Smith, N. J. Doran, F. M. Knox, and W. Forysiak, Opt. Lett. **21**, 1981 (1996).
[19] A. Hasegawa and Yu. Kodama, *Solitons in Optical Communications* (Oxford University Press, Oxford, 1995).
[20] V. I. Karpman, Phys. Scr. **20**, 462 (1978).
[21] L. D. Landau and E. M. Lifshitz, *Mechanics* (Pergamon, New York, 1975).
[22] H. Goldstein, *Classical Mechanics* (Wiley, New York, 1965).
[23] E. Hairer, S. P. Norsett, and G. Wanner, *Solving Ordinary Differential Equations I* (Springer-Verlag, Berlin, 1987).
[24] W. Press, B. Flannery, S. Teukolsky, and W. Vetterling, *Numerical Recipes, the Art of Scientific Computing* (Cambridge University Press, New York, 1986).
[25] N. B. Delone, V. P. Krainov, and D. L. Shepelyansky, Usp. Fiz. Nauk. **140**, 355 (1983) [Sov. Phys. Usp. **26**, 551 (1983)].
[26] B. V. Chirikov, Phys. Rep. **52**, 263 (1979).
[27] A. J. Lichtenberg and M. A. Lieberman *Regular and Stochastic Motion* (Springer-Verlag, Heidelberg, 1983).
[28] G. M. Zaslavsky and R. Z. Sagdeev, *Introduction to Nonlinear Physics* (Nauka Publishers, Moscow, 1988) (in Russian).
[29] B. A. Malomed, Opt. Commun. **136**, 313 (1997).
[30] T. S. Yang and W. Kath, Opt. Lett. **22**, 985 (1997).